

RESEARCH ARTICLE

A Distributed Algorithm for Controlling Continuous and Discrete Variables in a Radial Distribution Grid

JONATAN RALF AXEL KLEMETS¹ AND MERKEBU ZENEBE DEGEFA²

¹SINTEF Energy Research, 7034 Trondheim, Norway

Corresponding author: Jonatan Ralf Axel Klemets (jonatan.klemets@sintef.no)

This work was supported in part by the Centre for intelligent electricity distribution (CINELDI), an 8-years' Research Centre through the FME-scheme (Centre for Environment friendly Energy Research) under the grant 257626/E20; in part by The Research Council of Norway; in part by the CINELDI partners; and in part by the MultiGrid project, funded by the Department of Science and Technology in India under the grant INT/NOR/RCN/P-04/2019 along with the Research Council of Norway under the grant 285180.

ABSTRACT The increased integration of distributed energy resources (DERs) in the distribution network with intermittent generation profiles will likely make voltage regulation a difficult task. However, DERs bring both challenges and opportunities, as they can provide renewable forms of local energy and act as voltage regulating components. The DERs are usually interfaced with power electronic devices, in which both their active and reactive power outputs can be regulated and treated as continuous control variables. In contrast, other voltage regulatory devices such as On-Load Tap-Changing (OLTC) transformers are often controlled by making discrete tap changes. Thus, appropriate control strategies are required to control and coordinate the DERs with other voltage regulatory devices. In this work, a distributed control strategy based on the Alternating Direction Method of Multipliers (ADMM) is developed, which controls both the continuous and the discrete variables in a distribution grid. The proposed control strategy is compared to a centralized and a local control architecture, where optimal parameters have been computed for the local controllers. Finally, a simulation study is made for the three different control architectures using a modified CIGRE medium voltage network. The results showed significant improvements in the daily voltage profiles while also reducing the power losses by over 30% when using an optimal control strategy.

INDEX TERMS Voltage control, optimal control, distributed control, optimal power flow, reactive power.

I. INTRODUCTION

The transmission systems operators (TSOs) have traditionally been in charge of generating and supplying the necessary active and reactive power, mainly through coordinating different synchronous generators and compensator units [1]. However, the expected increase in distributed energy resources (DERs) and localized renewable energy sources (RES) is likely going to cause more voltage fluctuations in the grid. Thus, the distribution system operators (DSOs) will have to take a more active role in controlling the voltage and reducing large variations in the power flows at the DSO-TSO connection [1], [2]. Furthermore, as reactive

power sources connected to the transmission network are replaced by DERs in the distribution network, coordinated control will be necessary to reduce losses and achieve optimal operation.

The distribution system has primarily been a passive network, with seasonally changing tap settings of the On-Load Tap-Changing (OLTC) transformers being one of the main methods for local voltage control [3]. As a result, voltage and reactive power control in the distribution system have been done largely independently from each other [4]. However, with the adoption of more inverter-based DERs, it becomes important to properly control and coordinate these to ensure a stable voltage profile [5]. Thus, it becomes necessary to consider the regulation of the reactive power flow, while controlling the bus voltage levels and coordinating DERs with

The associate editor coordinating the review of this manuscript and approving it for publication was Turgay Celik¹.

other voltage regulating network components (such as OLTC, capacitor banks etc). Additionally, there will be a need for coordination among DSOs and TSO as they have their own objectives, control variables, and data security concerns.

Different control strategies have been proposed for the distribution system, but there are still many challenges that need to be addressed. These include proper selection of control architectures, adequate parameter settings of local controllers, and the cost-effective coordination of a large number of DERs. In [4], proper selection and trade-off of different control architectures is identified as one of the major challenges in voltage control. The communication bandwidth, latency, and the scalability of a centralized control architecture limit the ability of DERs from being engaged as active resources [6]. Instead, in most of the reviewed literature, the best outcome is anticipated through a combination of centralized, distributed, and decentralized control systems dispersed throughout the distribution network [7], [8]. Nevertheless, the barriers for practical implementation for the different architectures are not well-understood [9].

Distributed control has received significant attention in the research literature with several recent review papers [7], [10], [11]. Both centralized and distributed control strategies are able to achieve optimal operation. However, distributed control comes with several potential benefits over centralized control, such as reduced computational requirements, fewer communication lines, and safer sharing of personal data [11]. Most distributed algorithms tend to apply some augmented Lagrangian decomposition method [7], [10]. Out of these methods, the Alternating Direction Method of Multipliers (ADMM) is one of the most popular and has been studied in, e.g., [12], [13], [14], and [15]. In [16], a matrix-based formulation was used to implement an ADMM based multi-agent system on a cyber Hardware-in-the-Loop platform.

Most of the distributed control and ADMM algorithms that have been proposed for distribution systems only consider continuous variables for inverter-based DERs. However, many voltage regulation devices in the distribution grid consist of switches and tap changes which are discrete variables. Unfortunately, including discrete control from, e.g., On-Load Tap-Changing (OLTC) transformers can cause convergence issues for the ADMM algorithm, which was demonstrated in [14].

The optimal operation of local energy communities using ADMM was investigated in [17], which included both discrete and continuous variables. Binary variables were included in the local optimization problems to enforce that energy could not be sold and bought simultaneously. As a result, the value of the binary variables did not impact the cost of the optimal solution, which would not be applicable for controlling voltage regulation devices. A novel distributed voltage control strategy was proposed in [18], where each node follows a rule-based algorithm to determine the best trade-off between a local and a global objective to avoid violating the voltage constraints. However, rule-based algorithms may not be optimal, and it is difficult

to include other objectives, such as minimizing line losses. Deep reinforcement learning was used in [19] to create a model-free and distributed control algorithm for controlling switchable capacitor banks, voltage regulators, and different DERs. It was demonstrated that distributed control algorithms could be designed to reduce system losses and regulate the voltages similarly to a centralized control structure. However, an accurate model is required to learn the optimal control policies, and it is difficult to know how it will perform during unexpected events.

More recently, the Alternating Direction Inexact Newton algorithm (ALADIN) method has been proposed for solving distributed optimal power flow problems [20]. ALADIN resembles ADMM but can also guarantee convergence to a local optimum for non-convex problems and has been shown to converge faster than ADMM [21]. However, the ALADIN method relies on an update step that requires a central coordination controller and is, thus, not a fully distributed control algorithm. Similarly, a centralized ADMM algorithm was developed in [22] for solving mixed-integer nonlinear problems (MINLP) for distribution systems.

Distributed control algorithms based on ADMM that handles both discrete and continuous variables have been developed in [23], [24], [25], and [26]. Second-order cone programming (SCOP) combined with a branch and bound method was used in [23] to control the tap positions of the step voltage regulators and other DERs. However, it requires that the step voltage regulators are located on the shared branches between the adjacent control areas, and the algorithm could not dispatch other discrete variables, such as switched capacitor banks. Two ADMM algorithms were used in [24], first to find the approximate values for the discrete variables and then repeat the ADMM to find the continuous variables. A two-stage algorithm was developed in [25], where an outer loop was added to the ADMM algorithm. The inner ADMM loop can be solved in closed form, whereas the outer loop uses an interior-point method, with the model being linearized by perturbing it for each iteration. Another two-stage approach was proposed in [26]. The algorithm combines model predictive control with ADMM, with the discrete variables being solved and updated at a slower time scale compared to the continuous variables.

A. CONTRIBUTION

ADMM-based distributed controllers for both discrete and continuous have been developed in [23], [24], [25], and [26]. These methods incorporate additional layers and functions to the ADMM and show improvements in the performance and convergence of the distributed controllers. They also increase the individual controllers' complexity and computational burden by requiring appropriate solvers and additional optimization algorithms. However, the individual nodes in the distribution grids often deploy cheap sensors with limited computational capacity. Consequently, implementing more advanced control algorithms and solvers can be difficult in many practical applications.

In this work, a distributed control system based on ADMM is designed to minimize the losses and voltage deviations in a distribution grid. In contrast to other existing work that focuses on optimal controller performance, the aim of this paper is to develop an algorithm that can easily be implemented and approximately solve a distributed optimization algorithm for discrete and continuous variables. A novel approach is proposed for incorporating discrete control variables into the ADMM algorithm by introducing two additional variables and expanding the augmented Lagrangian. This modification results in the ADMM algorithm becoming bilinear which can be solved iteratively. Thus, it tries to take advantage of the already existing iterative requirement of the ADMM, where the resulting optimization problems can be solved in closed form. Therefore, it can be more easily implemented in practical implementations, as in [16], but where also discrete variables can be included.

The proposed algorithm is evaluated against two other control strategies in a case study. Typically, distributed controllers are only compared to a centralized controller, even if a simpler local control strategy could potentially achieve similar performance [27]. Thus, for comparison purposes, both a centralized and a local control strategy are designed where the parameters for the local controllers have been optimized specifically for the simulated model.

In summary, the two main contributions of this paper are:

- An ADMM-based algorithm for distributed controllers with both continuous and discrete control variables. The resulting optimization problem can be solved with a closed form solution and can thus more easily be implemented in most control devices.
- A case study that compares the performances of centralized, local, and distributed controller architectures for voltage control in distribution networks.

B. PAPER STRUCTURE

The structure of the paper is as follows: Part II starts by providing some relevant background before describing the centralized, and local control strategies in the subsections II-A, and II-B, respectively. The proposed ADMM based distributed control algorithm is presented in section III and constitutes the main contribution of this work. In section IV, the simulation results are presented, with the final conclusions drawn in section V.

II. PROBLEM FORMULATION AND CONTROL STRATEGIES

For balanced radial distribution networks, the relationship between the voltage and the power flows can be given by the nonlinear *DistFlow* equations [28], [29], [30]:

$$P_{i \rightarrow j} = P_{j \rightarrow k} + P_j - p_j - r_{i,j} l_{i \rightarrow j} \tag{1}$$

$$Q_{i \rightarrow j} = Q_{j \rightarrow k} + Q_j - q_j - x_{i,j} l_{i \rightarrow j} \tag{2}$$

$$v_j = v_i - 2(r_{i,j} P_{i \rightarrow j} + x_{i,j} Q_{i \rightarrow j}) + (r_{i,j}^2 + x_{i,j}^2) l_{i \rightarrow j} \tag{3}$$

$$l_{i \rightarrow j} = \frac{P_{i \rightarrow j}^2 + Q_{i \rightarrow j}^2}{v_i} \tag{4}$$

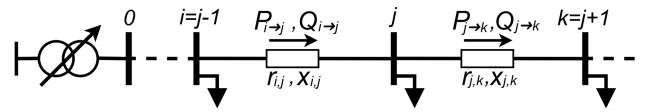


FIGURE 1. Schematic diagram of the DistFlow model for a radial network.

where $P_{i \rightarrow j}$, $Q_{i \rightarrow j}$, $r_{i,j}$, and $x_{i,j}$ are the active power flow, reactive power flow, line resistance, and line reactance between node i and j , respectively. The node voltage V_j is in (3) and (4) represented by its squared value, i.e., $v_j = V_j^2$. The DistFlow equations typically assume a unidirectional power flow, where the power flows to and from a node j as illustrated in Figure 1 with an OLTC located at node 0. Here, the upstream ($j - 1$) and the downstream ($j + 1$) nodes from node j have been denoted i and k , respectively. It will be assumed that the node connected to the OLTC behaves as a reference bus and that it is possible to provide the OLTC with different voltage setpoints. P_j is the active load, and Q_j is the reactive load at node j . Finally, if there are existing DERs in node j , then their active and reactive power generation is given by p_j , and q_j , respectively. Otherwise, p_j , and q_j will be equal to zero. Thus, the voltage in the grid can be controlled by p_j and q_j from different DERs or by using other voltage regulatory devices such as OLTCs [31].

The DistFlow equations in (1)–(4) can be made linear by neglecting the line losses such that $l_{i \rightarrow j} = 0$. Ignoring the losses will cause some model errors, but these are often considered to be relatively small [32]. The linearized DistFlow equations, are thus, given by

$$P_{i \rightarrow j} = P_{j \rightarrow k} + P_j - p_j \tag{5}$$

$$Q_{i \rightarrow j} = Q_{j \rightarrow k} + Q_j - q_j \tag{6}$$

$$v_j = v_i - 2(r_{i,j} P_{i \rightarrow j} + x_{i,j} Q_{i \rightarrow j}) \tag{7}$$

Ensuring that the voltage is kept within allowable limits is considered the main objective of the distribution grid. However, there exist several other objectives related to grid performance, e.g., minimizing voltage deviations, reducing active power losses, and load sharing between the DERs [10]. Based on the DistFlow models, the total voltage deviations from its setpoint v_j^{ref} can for a network with n -nodes be expressed as:

$$J_v = \sum_{j=0}^n (v_j - v_j^{ref})^2. \tag{8}$$

The power losses in the network can, as in [29], be approximated to

$$J_L \approx \sum_{i=0}^{n-1} r_{i,j} \frac{P_{i \rightarrow j}^2 + Q_{i \rightarrow j}^2}{v^{nom}} \tag{9}$$

with v^{nom} being the nominal voltage of the network. Finally, to encourage reactive power-sharing, a term of the total

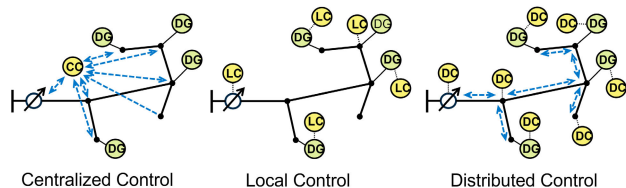


FIGURE 2. Centralized, local and distributed control architecture [10].

reactive power can be defined as

$$J_q = \sum_{j=1}^n q_j^2. \tag{10}$$

Achieving optimum for every objective is likely not feasible due to their conflicting nature, and thus, different priorities need to be assigned to them. Thus, it is necessary to use appropriate control strategies to avoid a sub-optimal performance. Based on the communication structure, the three main types of control system architectures are illustrated in Figure 2 and can be categorized as centralized, local, and distributed control [10].

A. CENTRALIZED CONTROL FORMULATION

Centralized control structures usually adopt a model-based optimization strategy, using some representation of the power flow equations [33]. Combining the model equations in (1)–(4) with the objectives in (8)–(10) results in the optimization problem:

$$\min_{P,Q,v,q} w_v J_v + w_L J_L + w_q J_q \tag{11}$$

$$\text{subject to (1), (2), and (3), } \forall j \in n, \tag{12}$$

$$q_j \leq \sqrt{s_j^2 - p_j^2}, \quad \forall j \in n, \tag{13}$$

$$v^{min} \leq v_0 \leq v^{max}, \tag{14}$$

where w_v , w_L , and w_q are scalar weights to assign different priorities on the objectives. It will be assumed that the generated active power p_j always is at its maximum value. Thus, the optimization problem in (11)–(14) solves for the reactive setpoints q_j and the voltage setpoint v_0 for the OLTC. As a result, q_j will be constrained in (13) by p_i and the apparent power capacity s_j of the inverter. Whereas v_0 in (14) is constrained by some upper v^{max} and lower v^{min} limits.

The setpoint v_0 will in (11)–(14) be treated as a continuous variable. However, the voltage at the OLTC will be influenced by its tap position, which is a discrete variable. Consequently, there may be a mismatch between the desired voltage v_0 and the actual voltage at the secondary side of the OLTC. This mismatch could be removed by representing the tap positions of the OLTC with discrete variables, but would result in a mixed-integer nonlinear programming problem (MINLP) that is difficult to scale.

B. LOCAL CONTROL FORMULATION

Local control solutions aim to control the DERs and the voltage regulatory devices solely based on local information. It was also demonstrated in [27] that a local control strategy could achieve similar performance to a centralized controller. However, the controllers in [27] was designed for reactive power dispatch in photovoltaic (PV) systems but did not consider different types of DERs or other voltage regulatory devices with discrete control variables. Therefore, a local control strategy based on rule-based control [34], [35] and droop controllers is proposed for controlling both DERs and OLTCs.

1) DROOP CONTROL FOR DERs

Droop controllers are often preferable for inverter-based DERs, where the reactive power injection is a controllable and continuous variable. For an inverter located at bus j , a volt-var droop control strategy can be given by

$$q_j = q_j^* + K_j (V_j^* - V_j) \tag{15}$$

Here, V_j^* and V_j are the target, and the measured voltage at node j , respectively. The target reactive power is denoted q_j^* and will, together with the droop gain K_j and the voltage difference determine the reactive power setpoint q_j . However, as in (13), the power output of an inverter will be constrained by its maximum apparent power s_j . Thus, to avoid having to reduce the active power produced, q_j will be restricted by

$$q_j^{max} := \sqrt{s_j^2 - p_j^2}. \tag{16}$$

As a result, the reactive power setpoint from the droop controller in (15) will be adjusted according to:

$$q_j = \begin{cases} -q_j^{max}, & \text{if } q_j \leq -q_j^{max} \\ q_j^{max}, & \text{if } q_j \geq q_j^{max} \\ q_j, & \text{otherwise.} \end{cases} \tag{17}$$

2) RULE-BASED CONTROL FOR OLTC TRANSFORMERS

The voltage levels in a radial network are dependent on the power flows, as seen in (3). Consequently, the voltage at the OLTC should be higher when the power demands are high to ensure all the voltages are kept above the allowed limit. Thus, a rule-based algorithm can be designed that sets the voltage at the OLTC based on the measured power flow.

Let P_T be the active power that flows through an OLTC transformer with N different tap positions. Assuming that the minimum voltage at the secondary side can be defined as V_0^{min} and that each tap position change corresponds to a voltage change given by ΔV . Then, by specifying some appropriate references for the active power flow $P_T^{ref,1} \dots P_T^{ref,N}$, a rule-based control strategy for computing the desired

voltage V_0 at the OLTC transformer can be formulated as

$$V_0 = \begin{cases} V_0^{min} + N\Delta V, & \text{if } P_T \geq P_T^{ref,N} \\ \vdots \\ V_0^{min} + 2\Delta V, & \text{if } P_T^{ref,3} > P_T \geq P_T^{ref,2} \\ V_0^{min} + 1\Delta V, & \text{if } P_T^{ref,2} > P_T \geq P_T^{ref,1} \\ V_0^{min}, & \text{otherwise.} \end{cases} \quad (18)$$

3) SELECTION OF THE LOCAL CONTROL PARAMETERS

The local controllers work autonomously without any complex communication structures. Therefore, it can often be assumed that the performance of local control strategies is not comparable to more advanced control structures. However, if the parameters K_j , q_j^* , V_j^* , and P_T^{ref} are chosen optimally, using, e.g., a meta-heuristic [36], or a surrogate modeling and optimization approach [37] then it could be possible to achieve similar performance to more complex control architectures. However, the local controllers are less flexible and may perform poorly when having to operate in different circumstances than they were originally designed for.

III. ADMM FOR DISTRIBUTED CONTROL

A distributed control structure consists of multiple local controllers that try to reach a consensus on the optimal operation of the network by communicating with its neighbors. Even though there is no need for a centralized controller, the distributed controllers are often designed based on the knowledge of the entire system. Thus, they work by decomposing, e.g., (11)–(14) into smaller sub-problems that can be solved locally by each distributed controller. Here, the proposed distributed controllers will be based on the Alternating Direction Method of Multipliers (ADMM). Therefore, a brief overview of ADMM will be presented next, but for a more detailed survey of ADMM and its applications, the reader is referred to [38].

A. ALTERNATING DIRECTION METHOD OF MULTIPLIERS (ADMM)

Alternating direction method of multipliers (ADMM) is an algorithm that solves optimization problems by partitioning the decision variables into two groups. The algorithm solves problems of the form:

$$\min_{y,z} f(y) + g(z) \quad (19)$$

$$\text{subject to } Ay + Bz = c, \quad (20)$$

where $y \in \mathbb{R}^{n_y}$, $z \in \mathbb{R}^{n_z}$, $A \in \mathbb{R}^{n_c \times n_y}$, $B \in \mathbb{R}^{n_c \times n_z}$, and $c \in \mathbb{R}^{n_c}$. The functions $f(\cdot)$ and $g(\cdot)$ are assumed to be convex and separable across the decision variable y and z . The ability to split the objective into two parts is what constitutes one of the main requirements of the ADMM method.

The problem in (19)–(20), can according to [38] be formulated as the scaled augmented Lagrangian,

$$\mathcal{L}_\rho(y, z, \Lambda) = f(y) + g(z) + \frac{\rho}{2} \|Ay + Bz - c + \Lambda\|_2^2 \quad (21)$$

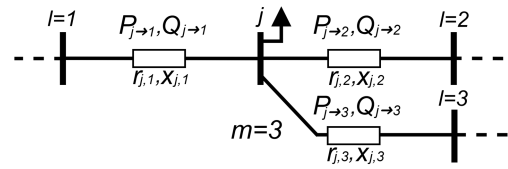


FIGURE 3. Power flows between node j and its three neighboring nodes.

where $\rho > 0$ is a penalty parameter, and Λ is an estimate of the the Lagrangian multiplier. The ADMM algorithm finds the solution to the problem in (19)–(20) by iteratively solving:

$$y = \arg \min_y f(y) + \frac{\rho}{2} \|Ay + Bz - c + \Lambda\|_2^2, \quad (22)$$

$$z = \arg \min_z g(z) + \frac{\rho}{2} \|Ay + Bz - c + \Lambda\|_2^2, \quad (23)$$

$$\Lambda = \Lambda + Ay + Bz - c. \quad (24)$$

Thus, the optimal y and z are solved in an alternating fashion, hence the name, alternating direction.

B. PROPOSED ADMM FORMULATION FOR DISTRIBUTED CONTROL

ADMM algorithms for distributed control based on the linearized DistFlow equations in (5)–(7) have previously been proposed in [29] and [30]. These assume that the power flows are unidirectional, i.e., that the location of the voltage source and the end nodes remain unchanged. However, in smart grids and self-healing networks, there may be a need to reroute the network, which could alter the power flow directions. Therefore, these distributed control algorithms will be modified to avoid having to assume a unidirectional power flow.

The linearized DistFlow equations in (5)–(7) can be generalized, as illustrated in Figure 3, such that for a node j with m neighboring nodes, they are given by

$$\sum_{l=1}^m P_{j \to l} = -P_j + p_j \quad (25)$$

$$\sum_{l=1}^m Q_{j \to l} = -Q_j + q_j \quad (26)$$

$$v_{lj} = v_j + 2(r_{j,l}P_{j \to l} + x_{j,l}Q_{j \to l}), \quad \forall l \in m. \quad (27)$$

Here, the subscripts for the voltages v_{lj} represent the voltage computed by the j :th node for its neighboring node l . The active and reactive power flows are similarly to the ones given in (5) and (6) with the subscripts in $P_{j \to l}$ and $Q_{j \to l}$ indicating the active and reactive power flows from node j to node l . As a result, the power flow direction is determined by its sign. A positive value means the power flows from l to j , whereas a flow is in the opposite direction will have a negative sign. Thus, the individual nodes do not require knowledge of the direction the voltage source v_0 is located at.

To ensure that the voltages v_j and v_{lj} correspond to the voltages computed at the neighboring nodes, the following

constraints must hold $\forall l \in m$:

$$v_j = v_{jl}, \quad v_{lj} = v_l, \quad (28)$$

where v_l , and v_{jl} are the voltages computed by the neighboring node l . Similarly, the power flow from node j to l must be equal its negative value from node l to j , such that $\forall l \in m$:

$$P_{j \rightarrow l} = -P_{l \rightarrow j}, \quad Q_{j \rightarrow l} = -Q_{l \rightarrow j}. \quad (29)$$

However, v_l , v_{jl} , $P_{l \rightarrow j}$, and $Q_{l \rightarrow j}$ in (28)–(29) will be computed by the neighboring node l , and can thus, not be included in the optimization problem for node j . Instead, local copies will be used that are denoted \hat{v}_l , \hat{v}_{jl} , $\hat{P}_{l \rightarrow j}$ and $\hat{Q}_{l \rightarrow j}$ for the neighboring variables. These variables will iteratively be updated until a consensus has been reached.

Based on (8), (9), and (10) an objective function for node j can be expressed as

$$J_j = \frac{\omega_v}{m+1} \left[(v_j - v_j^{ref})^2 + \sum_{l=1}^m (v_{lj} - v_l^{ref})^2 \right] + \frac{\omega_L}{2} \left[\sum_{l=1}^m r_{j,l} \frac{P_{j \rightarrow l}^2 + Q_{j \rightarrow l}^2}{v^{nom}} \right] + \omega_q q_j. \quad (30)$$

Here, the references v_l^{ref} for the neighboring nodes have been included in the objective function to improve the convergence of the ADMM algorithm. By dividing the voltage deviations, and active power losses with $m+1$, and 2, respectively, the sum of the objective in (30) for all nodes will equal the objective in (11) for the centralized controller.

Using (30) with (25)–(27) and the local copies, an optimization problem for node j can be formulated as

$$\min_{P_{j \rightarrow l}, Q_{j \rightarrow l}, v_{lj}, v_j, \hat{P}_{l \rightarrow j}, \hat{Q}_{l \rightarrow j}, \hat{v}_{jl}, \hat{v}_l, q_j} J_j \quad (31)$$

subject to (25), (26) and (27),

$$q_j \leq \sqrt{s_j^2 - p_j^2}, \quad (32)$$

$$v_{lj} = \hat{v}_l, \quad \forall l \in m, \quad (33)$$

$$v_j = \hat{v}_{jl}, \quad \forall l \in m, \quad (34)$$

$$P_{j \rightarrow l} = -\hat{P}_{l \rightarrow j}, \quad \forall l \in m, \quad (35)$$

$$Q_{j \rightarrow l} = -\hat{Q}_{l \rightarrow j}, \quad \forall l \in m. \quad (36)$$

The objective function in (31) and the constraints in (33)–(36) can as in (21) be expressed as the augmented Lagrangian:

$$\begin{aligned} \mathcal{L}_j = J_j + \frac{\rho}{2} \sum_{l=1}^m & \left[(v_j - \hat{v}_{jl} + \Lambda_l^{(vL)})^2 \right. \\ & + (v_{lj} - \hat{v}_l + \Lambda_l^{(vN)})^2 \\ & + (P_{j \rightarrow l} + \hat{P}_{l \rightarrow j} + \Lambda_l^{(P)})^2 \\ & \left. + (Q_{j \rightarrow l} + \hat{Q}_{l \rightarrow j} + \Lambda_l^{(Q)})^2 \right]. \quad (37) \end{aligned}$$

The proposed ADMM algorithm results in an iterative distributed control algorithm which after \hat{v}_{jl} , \hat{v}_l , $\hat{P}_{l \rightarrow j}$, $\hat{Q}_{l \rightarrow j}$,

$\Lambda_l^{(vL)}$, $\Lambda_l^{(vN)}$, $\Lambda_l^{(P)}$, and $\Lambda_l^{(Q)}$ have been initialized, follows the following steps:

- 1) **Local optimization:** For each node j solve the following optimization problem:

$$\min_{P_{j \rightarrow l}, Q_{j \rightarrow l}, v_{lj}, v_j, q_j} \mathcal{L}_j \quad (38)$$

subject to (25), (26), (27), and (32) (39)

Here, \hat{v}_{jl} , \hat{v}_l , $\hat{P}_{l \rightarrow j}$, $\hat{Q}_{l \rightarrow j}$, $\Lambda_l^{(vL)}$, $\Lambda_l^{(vN)}$, $\Lambda_l^{(P)}$, and $\Lambda_l^{(Q)}$ are given, and thus, (38)–(39) is a convex and quadratic optimization problem. The resulting values of v_{lj} , v_j , $P_{j \rightarrow l}$, and $Q_{j \rightarrow l}$ from solving (38)–(39), will be shared with the neighboring nodes in the next step.

- 2) **Share and update variables:** For each node j , collect v_l , v_{jl} , $P_{l \rightarrow j}$, and $Q_{l \rightarrow j}$ from all the $l \in m$ neighboring nodes and update the local copies:

$$\hat{v}_{lj} = \frac{1}{2} (v_{lj} + v_l), \quad \forall l \in m, \quad (40)$$

$$\hat{v}_j = \frac{1}{2} (v_j + v_{jl}), \quad \forall l \in m, \quad (41)$$

$$\hat{P}_{l \rightarrow j} = \frac{1}{2} (P_{j \rightarrow l} - P_{l \rightarrow j}), \quad \forall l \in m, \quad (42)$$

$$\hat{Q}_{l \rightarrow j} = \frac{1}{2} (Q_{j \rightarrow l} - Q_{l \rightarrow j}), \quad \forall l \in m. \quad (43)$$

- 3) **Update Lagrangian multipliers:** For node j , update the Lagrangian multipliers according to

$$\Lambda_l^{(vL)} = \Lambda_l^{(vL)} + v_j - \hat{v}_{jl}, \quad \forall l \in m, \quad (44)$$

$$\Lambda_l^{(vN)} = \Lambda_l^{(vN)} + v_{lj} - \hat{v}_l, \quad \forall l \in m, \quad (45)$$

$$\Lambda_l^{(P)} = \Lambda_l^{(P)} + P_{j \rightarrow l} + \hat{P}_{l \rightarrow j}, \quad \forall l \in m, \quad (46)$$

$$\Lambda_l^{(Q)} = \Lambda_l^{(Q)} + Q_{j \rightarrow l} + \hat{Q}_{l \rightarrow j}, \quad \forall l \in m. \quad (47)$$

Iteratively repeating the above steps will guarantee that the ADMM algorithm converges to the optimal solution as long as the problem is convex. Thus, the resulting the distributed controllers will give the same results as the centralized controller in (11) if the linearized DistFlow equations in (5)–(7) were used instead of (1)–(4). A closed form solution can also be derived for (38)–(39) for the ADMM algorithm. However, it results in a large expression and will not be shown here.

The primal and dual residuals are often used to determine when to terminate the iterative process of the ADMM [23], [38]. However, in practical implementations, a more straightforward approach is to set the number of iterations to a value that is sufficiently large to ensure convergence [16]. As long as the distributed controllers stay synchronized and run in parallel, they will update the setpoints simultaneously after the final iteration.

C. INCORPORATING BINARY VARIABLES WITH ADMM

The ADMM algorithm in the previous section is only applicable for nodes with inverter-based DERs and nodes that are not connected to the OLTC. For the node at the OLTC, the optimization problem in (38)–(39) can be modified to also include v_0 and the constraint in (14). However, this will result

in a sub-optimal solution since the resulting voltage setpoint will be a continuous variable, whereas the actual voltage of the OLTC will be influenced by its bandwidth ΔV . Thus, an alternative method will be proposed.

Let V_m be the voltage measurement at the secondary side of the OLTC and $V_0 = \sqrt{v_0}$ its voltage setpoint. The OLTC will make a tap change if the difference between the V_0 and V_m is greater than the bandwidth ΔV . Thus, two binary variables b^- and b^+ are defined that represent a tap decrease and a tap increase, respectively. Consequently, a tap change for the OLTC corresponds to the squared voltage v_0 according to

$$v_0 = b^-(V_m - \Delta V)^2 + b^+(V_m + \Delta V)^2 \quad (48)$$

Assuming that b^- and b^+ can not both be active at the same time, then the voltage at the OLTC with or without a tap change can be given by

$$v_0 = V_m^2 + b^-(\Delta V^2 - 2 V_m \Delta V) + b^+(\Delta V^2 + 2 V_m \Delta V). \quad (49)$$

The optimization problem in (38)–(39), can thus, be modified to include (49) and the binary variables b^- , and b^+ :

$$\min_{P_{j \rightarrow l}, Q_{j \rightarrow l}, v_{lj}, v_j, q_j, b^-, b^+} \mathcal{L}_j + \omega_b (b^- + b^+) \quad (50)$$

$$\text{subject to (25), (26), (27), and (49),} \quad (51)$$

$$b^{(-)} + b^{(+)} \leq 1 \quad (52)$$

Here, a small scalar weight ω_b has been included in the objective to avoid changing taps in the OLTC too frequently. The constraint in (52) ensures that b^- and b^+ can not be active at the same time. However, using binary variables with the ADMM algorithm can be problematic, primarily due to two reasons. First, the ADMM method is only guaranteed to converge for convex problems. Secondly, even in the case of convergence, it often results in a greedy algorithm, i.e., the binary variable will converge to a local optimum, which is often sub-optimal. Therefore, a different formulation is proposed, where the binary variables are replaced with continuous variables.

It has been well-established that binary variables can be transformed into continuous variables by constraining the variables such that [39]:

$$b^- - b^- b^- = 0, \quad b^+ - b^+ b^+ = 0. \quad (53)$$

Similarly, the constraint in (52) is equivalent to

$$b^- b^+ = 0. \quad (54)$$

The constraints in (53)–(54) are nonlinear, and thus, at first, glance does not seem to simplify the problem. However, by introducing two additional variables \hat{b}^- and \hat{b}^+ , the constraints in (53)–(54) can be rewritten as

$$b^- - b^- \hat{b}^- = 0, \quad b^+ - b^+ \hat{b}^+ = 0, \quad (55)$$

$$b^- \hat{b}^+ = 0, \quad b^+ \hat{b}^- = 0, \quad (56)$$

$$b^- = \hat{b}^-, \quad b^+ = \hat{b}^+. \quad (57)$$

The resulting constraints in (55)–(57) are bilinear and can be solved iteratively between $\{b^-, b^+\}$ and $\{\hat{b}^-, \hat{b}^+\}$. Therefore, it fits well with the ADMM algorithm since it already solves the optimization problem iteratively.

Defining:

$$\begin{aligned} \mathcal{L}^b & := \frac{\rho^b}{2} (b^- \hat{b}^+ + \Lambda^{(b^- b^+)})^2 + \frac{\rho^b}{2} (b^+ \hat{b}^- + \Lambda^{(b^+ b^-)})^2 \\ & + \frac{\rho^b}{2} (b^- - b_i^- \hat{b}^- + \Lambda^{(b^-)})^2 + \frac{\rho^b}{2} (b^+ - b_i^+ \hat{b}^+ + \Lambda^{(b^+)})^2 \\ & + \frac{\rho^b}{2} (b^- - \hat{b}^- + \Lambda^{(b^-)})^2 + \frac{\rho^b}{2} (b^+ - \hat{b}^+ + \Lambda^{(b^+)})^2 \end{aligned} \quad (58)$$

then for the node with the OLTC, the steps for the proposed ADMM algorithm can be adapted such that:

- 1) **Local optimization:** For node j , solve the following optimization problem:

$$\min_{P_{j \rightarrow l}, Q_{j \rightarrow l}, v_{lj}, v_j, q_j, v_0, b^-, b^+} \mathcal{L}_j + \mathcal{L}^b + \omega_b (b^- + b^+) \quad (59)$$

$$\text{subject to (25), (26), (27), (32), and (49)} \quad (60)$$

- 2) **Share and update variables:** For node j , collect $v_l, v_{jl}, P_{l \rightarrow j}$, and $Q_{l \rightarrow j}$ for all the $l \in m$ neighboring nodes and update the local copies as in (40)–(43). Next, update \hat{b}^- and \hat{b}^+ according to

$$\hat{b}^- = - \frac{b^+ \Lambda^{b^+ b^-} - b^- - \Lambda^{b^-} - b^- \Lambda^{b^- b^-} - (b^-)^2}{1 + (b^-)^2 + (b^+)^2} \quad (61)$$

$$\hat{b}^+ = - \frac{b^- \Lambda^{b^- b^+} - b^+ - \Lambda^{b^+} - b^+ \Lambda^{b^+ b^+} - (b^+)^2}{1 + (b^-)^2 + (b^+)^2} \quad (62)$$

Here, (61) and (62) are the closed form expressions for the optimal solution of (58) with respect to \hat{b}^- and \hat{b}^+ .

- 3) **Update Lagrangian multipliers:** For node j , update the Lagrangian multipliers as in (63)–(68) and then update the Lagrangian multipliers for the binary variables:

$$\Lambda^{(b^-)} = \Lambda^{(b^-)} + b^- - b^- \hat{b}^- \quad (63)$$

$$\Lambda^{(b^+)} = \Lambda^{(b^+)} + b^+ - b^+ \hat{b}^+ \quad (64)$$

$$\Lambda^{(b^- b^-)} = \Lambda^{(b^- b^-)} + b^- - \hat{b}^- \quad (65)$$

$$\Lambda^{(b^+ b^+)} = \Lambda^{(b^+ b^+)} + b^+ - \hat{b}^+ \quad (66)$$

$$\Lambda^{(b^- b^+)} = \Lambda^{(b^- b^+)} + b^- \hat{b}^+ \quad (67)$$

$$\Lambda^{(b^+ b^-)} = \Lambda^{(b^+ b^-)} + b^+ \hat{b}^- \quad (68)$$

- 4) **Update the penalty parameter ρ_b :** Based on the current value \mathcal{L}^b and its value from the previous iteration

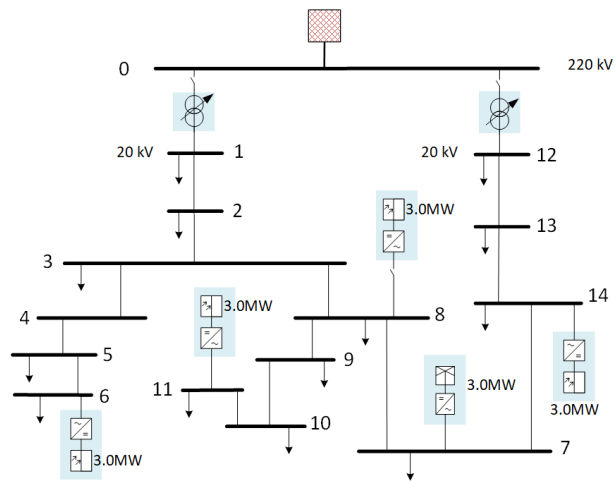


FIGURE 4. Modified CIGRE MV network grid model [41].

\mathcal{L}_{prev}^b , update the binary penalty parameter (ρ_b) according to

$$\rho_b = \begin{cases} \tau \rho_b, & \text{if } \mathcal{L}_{prev}^b - \mathcal{L}^b \geq \epsilon \\ \rho_b, & \text{otherwise} \end{cases} \quad (69)$$

where $1 \gg \epsilon \geq 0$, and $\tau > 1$.

For non-convex problems, convergence is only guaranteed for the ADMM algorithm if the penalty parameter is chosen sufficiently large [40]. Consequently, ρ_b must be chosen large enough to ensure convergence of the proposed algorithm. However, too large values for ρ_b often results in a sub-optimal solution since the algorithm will prioritize satisfying the constraints in (55)–(57) over minimizing the main objective in (50). Initializing ρ_b with a small value and updating it according to (69) has shown to give good results as it allows the algorithm to first prioritize the main objective before being forced to converge by satisfying the binary constraints.

IV. CASE STUDY

The three different control strategies are implemented and simulated on a modified CIGRE medium voltage network [41]. The model topology consists of 14 different busses as shown in Figure 4, where the busses 1 and 12 are connected to a 220 kV line through two separate OLTCs. Figure 5 shows the 24 hour load profiles for the different busses. Node 6, 7, 8, 11, and 14 are connected to some local power generation, where their 24 hour generation profiles are shown in Figure 6. These consist of four PV systems and one wind turbine, where each of them is interfaced through an inverter with a maximum capacity of 3.0 MVA. During the middle of the day, the total power generation will exceed the total load demand, whereas later in the day, the opposite is true. Thus, the controllers' ability to control the voltages and line losses with changing power flow directions can be evaluated.

Two different cases are simulated for each control strategy, wherein case 1, the OLTC at bus 12, has been deactivated by opening its associated switch. In case 2, the OLTC at

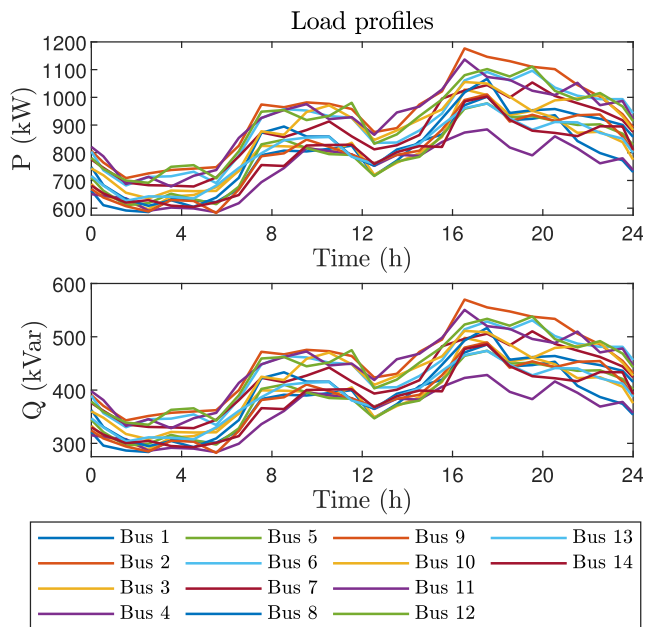


FIGURE 5. Daily load profiles at the different busses for the CIGRE network.

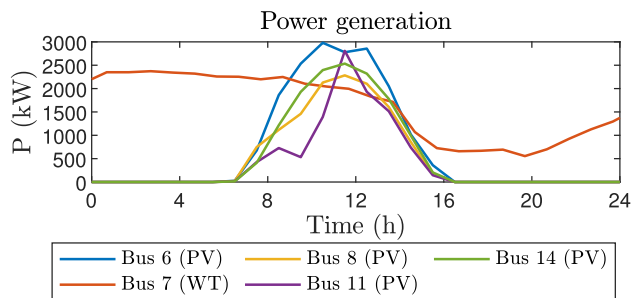


FIGURE 6. Generated power for a 24h period by the PV systems and wind turbine (WT), located at bus 6, 7, 8, 11, and 14, respectively.

bus 12 will be active while the OLTC at bus 1 has been taken out of service. This is to demonstrate the adaptability of the different control strategies when there is a need for rerouting the network caused by, e.g., a fault. Additionally, in case 2, the PV system at node eight has been taken out of commission. Consequently, there will be less local power production in case 2, and the direction of the power flows will differ compared to case 1.

The objective of the controllers is to minimize the voltage deviations and the active power losses in the network by controlling the OLTC and using the reactive power available at the DERs. The local control strategy has been optimized for case 1 using the method in [37] by simulating the grid model and the expected load and power generation for multiple sets of controller parameters.

A. SIMULATION RESULTS FOR CASE 1

The three different control architectures were each simulated for a 24 hour period. The resulting average voltages for the

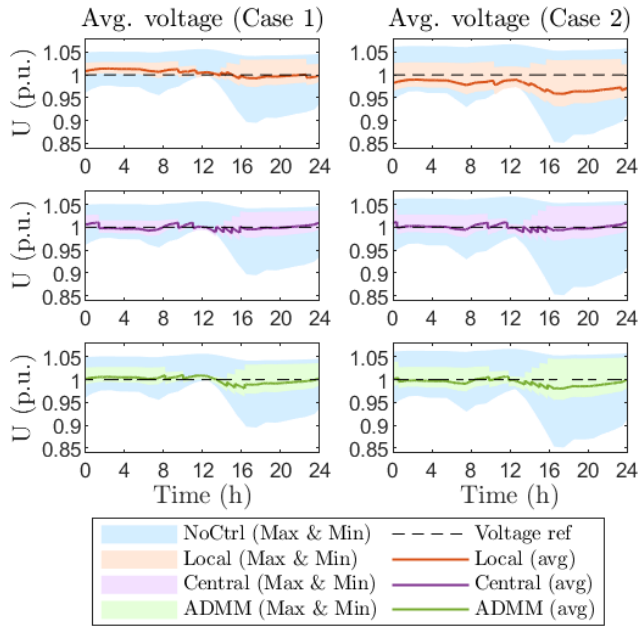


FIGURE 7. The average voltages together with their maximum and minimum voltages when using the local, centralized (central), and distributed (ADMM) control architectures. The blue area shows the maximum and minimum voltages when the network is left uncontrolled (NoCtrl), with the black dashed line being the desired voltage reference for the network.

grid, together with the minimum and maximum values, are shown in Figure 7. The voltages for each control strategy are compared to the maximum and minimum voltages when all the DERs and OLTC are left uncontrolled (No Ctrl) to highlight the advantage of using the control strategies. However, as seen in Figure 7, there are little differences in the voltage performance between the local, central, and distributed (ADMM) controllers. Similarly, when comparing the active power losses in Figure 8, all three control strategies give significant improvement to having no control. However, the difference between the three control systems is almost negligible.

The voltage setpoints sent to the OLTC are shown in Figure 9. Here, the centralized controller treats the voltage setpoint for the OLTC as a continuous variable, and thus, there is a disparity between the setpoint and the actual measured value. Similarly, the local controller computes the voltage setpoint based on the active power that flows through the OLTC, which also causes a voltage error. However, the ADMM algorithm uses binary variables to ensure a setpoint change is equal to the bandwidth of the OLTC. Thus, the ADMM will determine when a setpoint change is necessary or if the setpoint should be equal to the measured voltage. As a result, the voltage setpoint from the ADMM will almost perfectly match the measured voltage at the OLTC, which reduces the model error compared to the centralized controller.

The voltage setpoint from the ADMM is also compared to the optimal setpoint when using the linearized DistFlow model with binary variables as a centralized controller. The

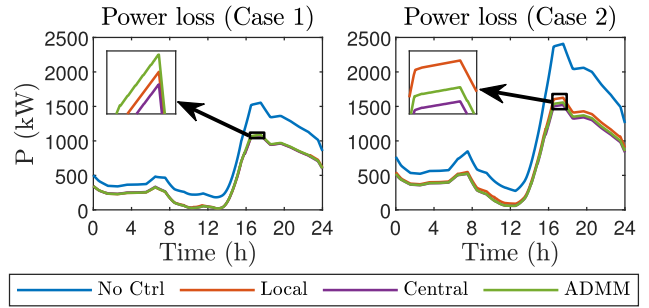


FIGURE 8. The active power losses when using the local, centralized (central), and distributed (ADMM) control architectures.

setpoints from the ADMM algorithm are almost equivalent to the optimal setpoints. The only exceptions are around the 8h, 10h, and 16h mark, where the ADMM will make a change about 10 minutes prior to the optimal setpoints. However, its impact on the performance will be negligible. Thus, suggesting that the proposed ADMM algorithm is capable of providing near-optimal setpoints.

Figure 10 shows the computed reactive power setpoints for the three different control systems. Despite some differences between the controllers, it does not significantly impact the performance related to the active power losses or the voltage deviations. Thus, showing that near-optimal performance can be achieved in multiple ways.

B. SIMULATION RESULTS FOR CASE 2

In case 2, the location of the voltage sources has changed from bus 1 to bus 12, and consequently, there will be a change in the direction of the power flows. Additionally, the PV system at bus 8 has been deactivated, and thus, it will not be able to provide any active or reactive power to the grid.

Both the centralized and the distributed ADMM control strategies are able to adapt to these changes and give similar improvements in the voltage, as seen in Figure 7. However, the voltage in case 2 for the local control strategy will deviate more than in case 1 since the controllers had been designed for case 1. Similarly, the active power losses in Figure 8 are slightly higher for the local controllers, whereas both the centralized and the distributed controllers give similar results. Nevertheless, despite the sub-optimal tuning of the local controllers, all three strategies are able to give significant improvements in both voltage deviations and power losses compared to having no control.

Finally, the voltage setpoints for the OLTC and the reactive power setpoints for the DGs are shown in Figure 9, and Figure 10, respectively. As in case 1, it can be seen that the voltage setpoints in Figure 9 for the centralized and local strategies will differ from the actual measured voltage values. Whereas the measured voltage will almost perfectly align with the setpoints from the ADMM algorithm. The optimal setpoint is, in this case, equivalent to the one computed by the ADMM, thus, demonstrating the effectiveness of the proposed method.

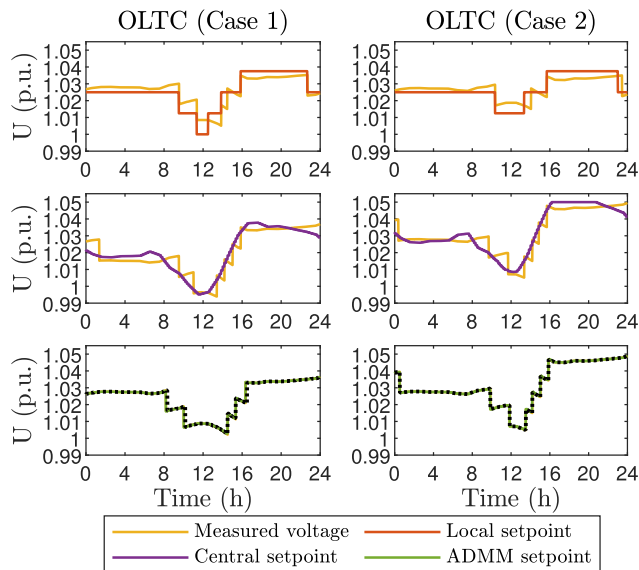


FIGURE 9. The measured voltage and the voltage setpoints for the OLTC using the local, centralized (central), and distributed (ADMM) control architectures. The black dotted lines represent the optimal setpoints to the OLTC when using a linearized DistFlow model with binary variables in a centralized controller.

C. SUMMARY OF THE SIMULATION RESULTS

The simulation results are summarized in Table 1, which shows the average voltage of the network with two standard deviations and the total active power losses for the two cases. The results from a centralized MINLP controller that uses continuous and discrete variables with the nonlinear model in (1)–(4) have also been included in Table 1 to use as a reference when comparing the performance of the different controllers. The centralized controller and the ADMM algorithm gives the best performance with the centralized controller slightly outperforming the ADMM algorithm due to its use of a nonlinear model. Therefore, in this case study, the model errors of using a linear model in the ADMM algorithm have a larger impact than the model errors for the central controller when using continuous variables for the OLTC step changes. However, if the voltage bandwidth for the OLTC had been larger or if there had been multiple other voltage regulatory devices with discontinuous properties, then the results may have been different. Nevertheless, both control strategies gave results close to the optimal MINLP controller.

Interestingly, the local control strategy is able to provide similar performance to the centralized and distributed control strategies. Especially in case 1 since controller parameters had been optimized for that simulation. However, the local control architecture is still able to give a significant improvement in the performance in case 2 compared to using no control. Thus, demonstrating the benefits of implementing some type of control strategy, even though it may not be optimal.

D. CONVERGENCE OF THE ADMM ALGORITHM

The generalized DistFlow equations used for the proposed ADMM algorithm will result in more decision variables com-

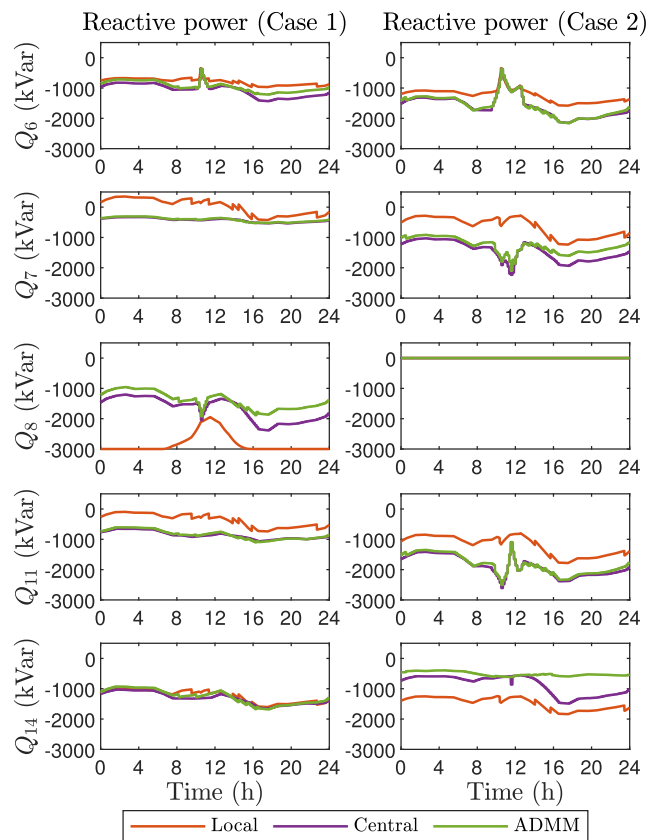


FIGURE 10. The injected reactive power to the grid at the different DGs when using the local, centralized (central), and distributed (ADMM) control architectures. Note that in case 2, the PV system at bus 8 has been deactivated, and thus, its reactive power output will be zero.

TABLE 1. Simulation results when using no (No Ctrl), local, centralized (central), and distributed (ADMM) control. The results are compared with an optimal algorithm that solves a MINLP problem.

	Case 1		Case 2	
	$\bar{U} \pm 2\sigma$	P_{loss}	$\bar{U} \pm 2\sigma$	P_{loss}
No Ctrl	0.977 ± 0.074	16.382	0.956 ± 0.100	25.689
Local	1.004 ± 0.023	10.654	0.978 ± 0.042	17.118
Central	1.000 ± 0.020	10.611	1.000 ± 0.027	15.986
ADMM	0.999 ± 0.024	10.672	0.993 ± 0.032	16.262
Optimal	0.999 ± 0.018	10.613	1.000 ± 0.026	15.928

pared to, e.g., the approach in [29]. As a consequence of having more decision variables, one would expect the convergence time to increase. However, by providing each node with the setpoints for the neighboring nodes, the proposed ADMM algorithm will have a similar convergence compared to [29], as shown in Figure 11. However, as previously addressed in [29] and [38], the convergence of the ADMM algorithm will be heavily influenced by the value on ρ .

Finally, the convergence properties of the proposed ADMM algorithm with binary variables are investigated. Here, the value of ρ will be kept constantly at 50 for all the nodes, but different values will be used for ρ_b . The convergence results can be seen in Figure 12 and show how

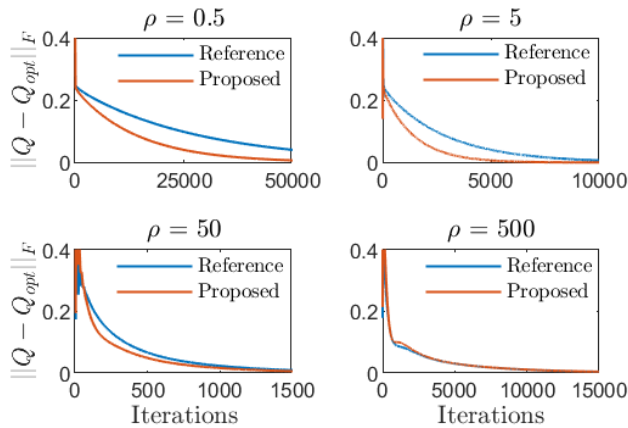


FIGURE 11. Convergence of the reactive power setpoints toward their optimal values for different values on ρ when comparing the proposed ADMM algorithm to the one in the reference [29]. Here, the voltage at the slack bus is constant, and thus, the binary variables have not been included.

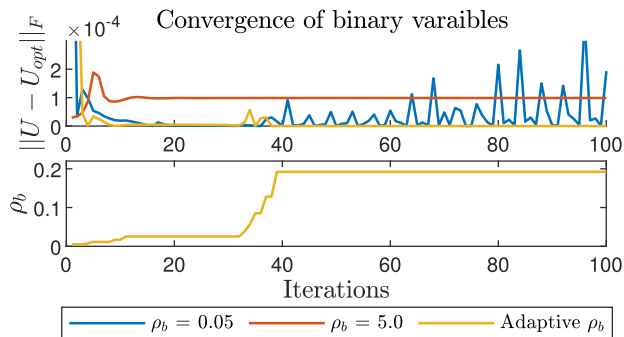


FIGURE 12. Convergence of the voltage setpoint for the OLTC towards its optimal value for different values on ρ_b .

different values of ρ_b influence the convergence. If the value is chosen too large, there is a high probability that the algorithm will converge to a sub-optimal solution. Choosing a too small value can cause the ADMM algorithm to become unstable and not converge, highlighting the challenge when using ADMM for non-convex problems. However, by using the proposed adaption method in (69), it is possible to reach convergence while also very frequently finding the optimal solution. This was also demonstrated in Figure 9, where voltage setpoints computed for the OLTC by the ADMM were almost identical to the optimal setpoints.

V. CONCLUSION

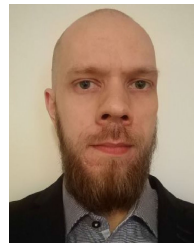
A centralized, local, and distributed control architecture have been designed for voltage control and loss reduction in a distribution network. The main focus has been on distributed controllers, where a novel method for incorporating discrete variables in the ADMM algorithm is presented. Compared to other works, the distributed optimization problem can approximately be solved in closed form, which makes it easier to implement in most control devices.

All three control architectures showed significant reductions in voltage deviations and active power losses compared to having no control. However, the control strategies gave very similar performances, demonstrating that near-optimal control can be achieved in multiple ways. Thus, it suggests that the best control structure will be case-specific, where more emphasis should be put on, e.g., ICT infrastructure, scalability, needs for reconfiguration, and resilience towards cyberattacks and different types of disturbances when choosing the control architecture. Future works will investigate the challenges related to those three aspects together with cyber-physical testing of the different control architectures in a more realistic laboratory environment.

REFERENCES

- [1] D. Stock, F. Sala, A. Berizzi, and L. Hofmann, "Optimal control of wind farms for coordinated TSO-DSO reactive power management," *Energies*, vol. 11, no. 1, p. 173, Jan. 2018.
- [2] J. Morin, F. Colas, X. Guillaud, S. Grenard, and J.-Y. Dieulot, "Rules based voltage control for distribution networks combined with TSO-DSO reactive power exchanges limitations," in *Proc. IEEE Eindhoven PowerTech*, Jun. 2015, pp. 1–6.
- [3] V. Ilea, C. Bovo, D. Falabretti, M. Merlo, C. Arrigoni, R. Bonera, and M. Rodolfi, "Voltage control methodologies in active distribution networks," *Energies*, vol. 13, no. 12, p. 3293, Jun. 2020.
- [4] H. Sun, Q. Guo, J. Qi, V. Ajjarapu, R. Bravo, J. Chow, Z. Li, R. Moghe, E. Nasr-Azadani, U. Tamrakar, G. N. Taranto, R. Tonkoski, G. Valverde, Q. Wu, and G. Yang, "Review of challenges and research opportunities for voltage control in smart grids," *IEEE Trans. Power Syst.*, vol. 34, no. 4, pp. 2790–2801, Jul. 2019.
- [5] F. Hinz and D. Most, "The effects of reactive power provision from the distribution grid on redispatch cost," in *Proc. 13th Int. Conf. Eur. Energy Market (EEM)*, Jun. 2016, pp. 1–6.
- [6] K. P. Schneider, S. Laval, J. Hansen, R. B. Melton, L. Ponder, L. Fox, J. Hart, J. Hambrick, M. Buckner, M. Baggu, and K. Prabakar, "A distributed power system control architecture for improved distribution system resiliency," *IEEE Access*, vol. 7, pp. 9957–9970, 2019.
- [7] D. K. Molzahn, F. Dörfler, H. Sandberg, S. H. Low, S. Chakrabarti, R. Baldick, and J. Lavaei, "A survey of distributed optimization and control algorithms for electric power systems," *IEEE Trans. Smart Grid*, vol. 8, no. 6, pp. 2941–2962, Jul. 2017.
- [8] D. Messmer and K. Malmedal, "Optimizing distributed energy resource control system architecture," in *Proc. IEEE Rural Electr. Power Conf. (REPC)*, Apr. 2021, pp. 67–72.
- [9] A. Keane, L. F. Ochoa, C. L. T. Borges, G. W. Ault, A. D. Alarcon-Rodriguez, R. A. F. Currie, F. Pilo, C. Dent, and G. P. Harrison, "State-of-the-art techniques and challenges ahead for distributed generation planning and optimization," *IEEE Trans. Power Syst.*, vol. 28, no. 2, pp. 1493–1502, May 2013.
- [10] K. E. Antoniadou-Plytaria, I. N. Kouveliotis-Lysikatos, P. S. Georgilakis, and N. D. Hatzigiorgiou, "Distributed and decentralized voltage control of smart distribution networks: Models, methods, and future research," *IEEE Trans. Smart Grid*, vol. 8, no. 6, pp. 2999–3008, Nov. 2017.
- [11] Y. Wang, S. Wang, and L. Wu, "Distributed optimization approaches for emerging power systems operation: A review," *Electr. Power Syst. Res.*, vol. 144, pp. 127–135, Mar. 2017.
- [12] S. Magnússon, P. C. Weeraddana, and C. Fischione, "A distributed approach for the optimal power-flow problem based on ADMM and sequential convex approximations," *IEEE Trans. Control Netw. Syst.*, vol. 2, no. 3, pp. 238–253, Sep. 2015.
- [13] T. Erseghe, "Distributed optimal power flow using ADMM," *IEEE Trans. Power Syst.*, vol. 29, no. 5, pp. 2370–2380, Sep. 2014.
- [14] K. Christakou, D.-C. Tomozei, J.-Y. L. Boudec, and M. Paolone, "AC OPF in radial distribution networks—Part I: On the limits of the branch flow convexification and the alternating direction method of multipliers," *Electr. Power Syst. Res.*, vol. 143, pp. 438–450, Feb. 2017.
- [15] A. Maneesha and K. S. Swarup, "A survey on applications of alternating direction method of multipliers in smart power grids," *Renew. Sustain. Energy Rev.*, vol. 152, Dec. 2021, Art. no. 111687.

- [16] T.-L. Nguyen, Q.-T. Tran, R. Caire, Y. Wang, Y. Besanger, and N.-A. Luu, "Distributed optimal power flow and the multi-agent system for the realization in cyber-physical system," *Electr. Power Syst. Res.*, vol. 192, Mar. 2021, Art. no. 107007.
- [17] S. Lilla, C. Orozco, A. Borghetti, F. Napolitano, and F. Tossani, "Day-ahead scheduling of a local energy community: An alternating direction method of multipliers approach," *IEEE Trans. Power Syst.*, vol. 35, no. 2, pp. 1132–1142, Mar. 2020.
- [18] H. E. Z. Farag and El-Saadany, "A novel cooperative protocol for distributed voltage control in active distribution systems," *IEEE Trans. Power Syst.*, vol. 28, no. 2, pp. 1645–1656, May 2013.
- [19] H. Li, Z. Wang, and H. He, "Distributed volt-VAR optimization based on multi-agent deep reinforcement learning," in *Proc. Int. Joint Conf. Neural Netw. (IJCNN)*, Jul. 2021, pp. 1–7.
- [20] A. Engelmann, Y. Jiang, T. Muhlpofer, B. Houska, and T. Faulwasser, "Toward distributed OPF using ALADIN," *IEEE Trans. Power Syst.*, vol. 34, no. 1, pp. 584–594, Jan. 2019.
- [21] N. Meyer-Huebner, M. Suriyah, and T. Leibfried, "Distributed optimal power flow in hybrid AC–DC grids," *IEEE Trans. Power Syst.*, vol. 34, no. 4, pp. 2937–2946, Jul. 2019.
- [22] A. Alburidy and L. Fan, "An alternating direction method of multipliers-based approach to solve mixed-integer nonlinear volt/var optimization problems in distribution systems," *Int. Trans. Electr. Energy Syst.*, vol. 31, no. 3, pp. 1–23, 2021.
- [23] Y. Liu, L. Guo, C. Lu, Y. Chai, S. Gao, and B. Xu, "A fully distributed voltage optimization method for distribution networks considering integer constraints of step voltage regulators," *IEEE Access*, vol. 7, pp. 60055–60066, 2019.
- [24] F. U. Nazir, B. C. Pal, and R. A. Jabr, "Distributed solution of stochastic Volt/Var control in radial networks," *IEEE Trans. Smart Grid*, vol. 11, no. 6, pp. 5314–5324, Nov. 2020.
- [25] W. Lu, M. Liu, S. Lin, and L. Li, "Incremental-oriented ADMM for distributed optimal power flow with discrete variables in distribution networks," *IEEE Trans. Smart Grid*, vol. 10, no. 6, pp. 6320–6331, Nov. 2019.
- [26] Z. Li, Q. Wu, J. Chen, S. Huang, and F. Shen, "Double-time-scale distributed voltage control for unbalanced distribution networks based on MPC and ADMM," *Int. J. Electr. Power Energy Syst.*, vol. 145, Feb. 2023, Art. no. 108665.
- [27] K. Turitsyn, P. Sulc, S. Backhaus, and M. Chertkov, "Local control of reactive power by distributed photovoltaic generators," in *Proc. 1st IEEE Int. Conf. Smart Grid Commun.*, Oct. 2010, pp. 79–84.
- [28] M. E. Baran and F. F. Wu, "Optimal sizing of capacitors placed on a radial distribution system," *IEEE Trans. Power Del.*, vol. 4, no. 1, pp. 735–743, Jan. 1989.
- [29] P. Šulc, S. Backhaus, and M. Chertkov, "Optimal distributed control of reactive power via the alternating direction method of multipliers," *IEEE Trans. Energy Convers.*, vol. 29, no. 4, pp. 968–977, Dec. 2014.
- [30] S. Huang, P. Li, Q. Wu, F. Li, and F. Rong, "ADMM-based distributed optimal reactive power control for loss minimization of DFIG-based wind farms," *Int. J. Electr. Power Energy Syst.*, vol. 118, Jun. 2020, Art. no. 105827.
- [31] M. Z. Degefa, M. Lehtonen, R. J. Millar, A. Alahäivälä, and E. Saarijärvi, "Optimal voltage control strategies for day-ahead active distribution network operation," *Electric Power Syst. Res.*, vol. 127, pp. 41–52, Oct. 2015.
- [32] H. Zhu and H. J. Liu, "Fast local voltage control under limited reactive power: Optimality and stability analysis," *IEEE Trans. Power Syst.*, vol. 31, no. 5, pp. 3794–3803, Sep. 2016.
- [33] E. Dall'Anese and A. Simonetto, "Optimal power flow pursuit," *IEEE Trans. Smart Grids*, vol. 9, no. 2, pp. 942–952, Mar. 2018.
- [34] S. Teleke, M. E. Baran, S. Bhattacharya, and A. Q. Huang, "Rule-based control of battery energy storage for dispatching intermittent renewable sources," *IEEE Trans. Sustain. Energy*, vol. 1, no. 3, pp. 117–124, Oct. 2010.
- [35] T. Sansawatt, J. O'Donnell, L. F. Ochoa, and G. P. Harrison, "Decentralised voltage control for active distribution networks," in *Proc. 44th Int. Universities Power Eng. Conf.*, Sep. 2009, pp. 1–5.
- [36] J. Kennedy and R. C. Eberhart, "Particle swarm optimization," in *Proc. IEEE Int. Conf. Neural Netw.*, vol. 4, Perth, WA, Australia, Nov/Dec. 1995, pp. 1942–1948.
- [37] H.-M. Gutmann, "A radial basis function method for global optimization," *J. Global Optim.*, vol. 19, no. 3, pp. 201–227, 2001.
- [38] S. Boyd, N. Parikh, E. Chu, B. Peleato, and J. Eckstein, "Distributed optimization and statistical learning via the alternating direction method of multipliers," *Found. Trends Mach. Learn.*, vol. 3, no. 1, pp. 1–124, Nov. 2010.
- [39] P. L. Hammer and A. A. Rubin, "Some remarks on quadratic programming with 0–1 variables," *Revue Française d'informatique et de Recherche Opérationnelle. Série verte*, vol. 4, no. V3, pp. 67–79, 1970.
- [40] M. Hong, Z.-Q. Luo, and M. Razaviyayn, "Convergence analysis of alternating direction method of multipliers for a family of nonconvex problem," *J. Optim.*, vol. 26, no. 1, pp. 337–364, 2016.
- [41] *Benchmark Systems for Network Integration of Renewable and Distributed Energy Resources*, Task Force C6.04, CIGRÉ, Paris, France, 2014.



JONATAN RALF AXEL KLEMETS received the M.Sc. degree in advanced control and systems engineering from the University of Manchester, U.K., in 2013, and the Ph.D. degree in engineering cybernetics from the Norwegian University of Science and Technology (NTNU), Trondheim, Norway, in 2019. He is currently working as a Research Scientist at SINTEF Energy Research, Trondheim. His research interests include optimization and control for applications related to renewable energy, smart grids, and the electrification of transport.



MERKEBU ZENEBE DEGEFA received the M.Sc. degree in electrical engineering, in 2010, and the Ph.D. degree in power systems and high-voltage engineering from Aalto University, Espoo, Finland, in 2015. He is currently a Research Scientist at SINTEF Energy Research. He has authored more than 50 scientific papers. His research interests include the development of advance operational functions for active distribution systems, laboratory-based testing, the development of ancillary services, and load and flexibility modeling.

• • •